J. Am. Soc. Mass Spectrom. (2015) 26:1899–1902
DOI: 10.1007/s13361-015-1242-7

SHORT COMMUNICATION

Accurate Mass MS/MS/MS Analysis of Siderophores Ferrioxamine B and E1 by Collision-Induced Dissociation Electrospray Mass Spectrometry

Ashley M. Sidebottom,[1] Jonathan A. Karty,[1] Erin E. Carlson[1,2,3]

[1]Department of Chemistry, Indiana University, Bloomington, IN 47403, USA
[2]Department of Molecular and Cellular Biochemistry, Indiana University, Bloomington, IN 47403, USA
[3]*Present Address:* Department of Chemistry, University of Minnesota, 207 Pleasant St. SE, Minneapolis, MN 55455, USA

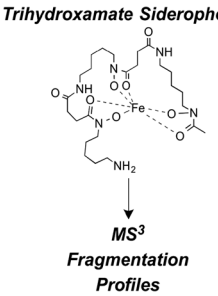

Abstract. Siderophores are bacterially secreted, small molecule iron chelators that facilitate the binding of insoluble iron (III) for reuptake and use in various biological processes. These compounds are classified by their iron (III) binding geometry, as dictated by subunit composition and include groups such as the trihydroxamates (hexadentate ligand) and catecholates (bidentate). Small modifications to the core structure such as acetylation, lipid tail addition, or cyclization, make facile characterization of new siderophores difficult by molecular ion detection alone (MS^1). We have expanded upon previous fragmentation-directed studies using electrospray ionization collision-induced dissociation tandem mass spectrometry (ESI-CID-MS/MS/MS) and identified diagnostic MS^3 features from the trihydroxamate siderophore class for ferrioxamine B and E1 by accurate mass. Diagnostic features for MS^3 include C–C, C–N, amide, and oxime cleavage events with proposed losses of water and –CO from the iron (III) coordination sites. These insights will facilitate the discovery of novel trihydroxamate siderophores from complex sample matrices.

Keywords: Siderophore, Trihydroxamate, MS/MS/MS, Accurate mass

Received: 14 April 2015/Revised: 17 July 2015/Accepted: 23 July 2015/Published Online: 1 September 2015

Introduction

Iron is an essential nutrient for bacteria and fungi; however, acquisition under aqueous, aerobic conditions is challenging because of the insolubility of iron (III). Microorganisms overcome this by chelating iron (III) with secreted siderophores for extracellular sequestration and uptake across cellular membranes [1]. Siderophores are low molecular weight compounds that have reported affinities for iron (III) between 10^{29} and 10^{43} M^{-1} [2]. Chelation occurs through oxygen coordination with characteristic subunits (e.g., trihydroxamate; Figure 1). In addition to common cellular processes that require iron as a cofactor (e.g., TCA cycle, DNA replication), siderophore-mediated iron acquisition aids in the virulence of organisms such as *Staphylococcus aureus* and *Pseudomonas aeruginosa* [3, 4]. To date, >500 siderophores have been discovered and despite their similar function, the structures vary widely, playing a major role in recognition by membrane-bound proteins and diffusion away from cellular membranes [5, 6]. Trihydroxamate siderophores are synthesized by nonribosomal peptide synthetase-independent synthetases (NISs) and commonly contain *N*-hydroxy-*N*-succinyl-cadaverine blocks [7]. Recent work, however, has revealed the high propensity for variable subunit incorporation, such as a lipid tail, desaturation event, or acetylation, modulating the bioactivity of these compounds [8, 9].

Previous CID fragmentation studies have provided diagnostic, nominal/accurate mass information for iron (III) bound and apo (unbound) siderophores at the MS and MS^2 level and include several common ferrioxamines such as B, G, D_2, and E (Figure 1a, b) [10–14]. The iron (III) unbound state is frequently more abundant in bacterial extracts and has therefore been more widely studied. However, recent MS-based studies discovered a suite of low abundance (~ng/L), iron (III) bound trihydroxamates, suggesting that additional iron bound siderophores remain to be analyzed [9]. In addition to fragmentation patterns similar to the ferrioxamines mentioned above, the iron (III) bound forms are readily identifiable because of the $^{54}Fe/^{56}Fe$ isotope ratio (6.4%

Electronic supplementary material The online version of this article (doi:10.1007/s13361-015-1242-7) contains supplementary material, which is available to authorized users.

Correspondence to: Erin Carlson; *e-mail:* carlsone@umn.edu

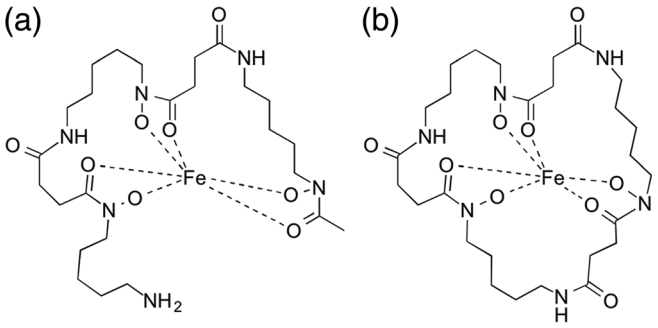

Figure 1. Structures of the trihydroxamate siderophores (**a**) ferrioxamine B (Fer B), and (**b**) ferrioxamine E1 (Fer E1)

Fe^{54}/100% Fe^{56}). For these reasons, the fragmentation patterns of these features, $[M - 2H + Fe]^+$, are of great significance for compound discovery as low abundant species represent an unexplored source of novel molecules.

In this work, recurrent fragmentation pathways have been characterized based on accurate tandem mass spectrometry (MS^2 and MS^3; positive mode; nano-LC-ESI-CID-LTQ-Orbitrap) analysis of a linear trihydroxamate siderophore, ferrioxamine B (Fer B), and cyclic ferrioxamine E1 (Fer E1), which were chosen for their similar scaffolds yet diverse fragmentation pathways. Diagnostic fragmentation pathways were confirmed with accurate masses observed in MS^2 studies and proposed at the MS^3 level. We sought to characterize these ion chemistries for the future elucidation of unique subunit structures in previously uncharacterized, low abundant, iron-coordinated siderophores [9].

Materials and Methods

Desferrioxamine B and ferrioxamine E1 were purchased from Sigma-Aldrich (St. Louis, MO, USA) and diluted in MS-grade methanol (EMD) for analysis. Iron (III) chloride (Sigma-Aldrich) was added at 1 mg/mL to 0.5 mg/mL desferrioxamine B to produce chelated ferrioxamine B. Accurate mass data of the iron (III) bound form was acquired using nano-LC-ESI-linear ion trap quadrupole-Orbitrap (Thermo Scientific, Waltham, MA, USA, LTQ Orbitrap XL). Ions were fragmented with a normalized collision energy of 35.0, FT resolution 7500, and 30.0 ms activation time. The top three most abundant species were selected for MS^2 and subsequent MS^3 studies. Accurate mass spectra of precursor and fragment ions were acquired by the Orbitrap and spectra were then analyzed using Xcalibur processing software.

Results and Discussion

Linear, Ferrioxamine B, and Cyclized Ferrioxamine E1: MS^2

At the MS^2 level, all three major product ions of Fer B were observed with bound iron ($[M -2H + Fe]^+$) and detected with <6 ppm accuracy (SI Table 1, SI Figures 1 and 2) [11, 12]. Previously characterized diagnostic fragments were observed and include (m/z_o, observed value; m/z_t, theoretical value): m/z_o = 597.2486 ($-NH_3$), 496.1639 (hydroxamate cleavage between N7 and C8), and 414.1581 (amide cleavage between C11 and N12) [14]. Additional fragments were observed at lower abundance and smaller mass/charge ratios than the major cleavage events. Examples include the following (formulas match at <9 ppm): m/z_t = 397.1295, m/z_o = 397.1313 ($C_{16}H_{27}N_3O_5Fe^+$), m/z_t = 314.0560, m/z_o = 314.0583 ($C_{11}H_{18}N_2O_5Fe^+$), and m/z_t = 270.0661, m/z_o = 270.0678 ($C_{10}H_{18}N_2O_3Fe^+$). It is interesting to note that while most fragments result from cleavage at two positions, with loss of a monohydroxyl unit being typical, one fragment, m/z = 314.0560, retains a hydroxamate –OH as a (bis) Fe (III)-dihydroxamate species (SI Figure 3). This fragment has been previously observed, predominantly at low pH (<2) and at nominal mass accuracy [14, 15]. Fragments such as these can be expected to differ within suites of siderophores or novel compound structures.

The top three major MS^2 fragments of the cyclized siderophore, Fer E1 ($[M - 2H + Fe]^+$), were detected with <2 ppm accuracy (SI Table 1, SI Figures 4 and 5). Previously characterized, diagnostic fragments were observed and include: m/z_o = 636.2561 ($-H_2O$), 619.2297 (N(1)-C(2), C(33)-N(1), (N(7)-O)-Fe, and N(7)-O cleavage), and 537.2237 (C(6)-N(7), C(11)-N(12) and (N(7)-O)-Fe cleavage) (SI Figure 5) [11, 12]. Another species of interest, at m/z_t = 437.1244, resulted from cleavage at three positions: (1) between the α-methylene group (C2) and N(1), (2) the amide at C(22)-N(23), and (3) (N(29)-O)-Fe, accounting for the neutral loss of 217.1432 Da ($-C_9H_{19}N_3O_3$). This is especially informative because the linear Fer B cannot fragment in an analogous way because of the lack of a third amide and additional succinate equivalent as are found in Fer E1. Minor fragments observed include the following: m/z_t = 471.1775, m/z_o = 471.1773 ($C_{18}H_{33}N_5O_6Fe^+$), and m/z_t = 295.0745, m/z_o = 295.0740 ($C_{12}H_{10}N_2O_3Fe^+$) (SI Figure 4). As with Fer B, these ions map smaller regions of the Fer E1 structure and the masses of homologous fragments are expected to deviate for other compounds in this class.

Linear, Ferrioxamine B: MS^3

Prior to this report, MS^3 studies with accurate mass analysis have, to the best of our knowledge, not been performed on ferrioxamine B or E1. MS^3 was pursued for access to additional diagnostic fragments of Fer B. The three most abundant ions in the Fer B MS^2 spectrum (m/z = 597, 496, 414) were chosen for MS^3 analysis (±0.5 Da mass selection window) (SI Figure 1). The detected MS^3 fragments, proposed neutral losses, and ppm deviations are summarized in SI Tables 2 and 3. At the MS^3 level, dominant fragments were formed as a result of water ($-H_2O$; fragment *a*, Figure 2a), carbon monoxide (–CO; fragment *i*, Figure 2b), or carbon monoxide/water loss (–CO + $-H_2O$; fragment *o*, Figure 2c) from the molecular ion. Carbon monoxide loss was common for fragments containing terminal (–CO) species from previous MS^2 fragmentation. Additional neutral loss species can be found in SI Table 2. Despite the previously described structural variations observed between trihydroxamate

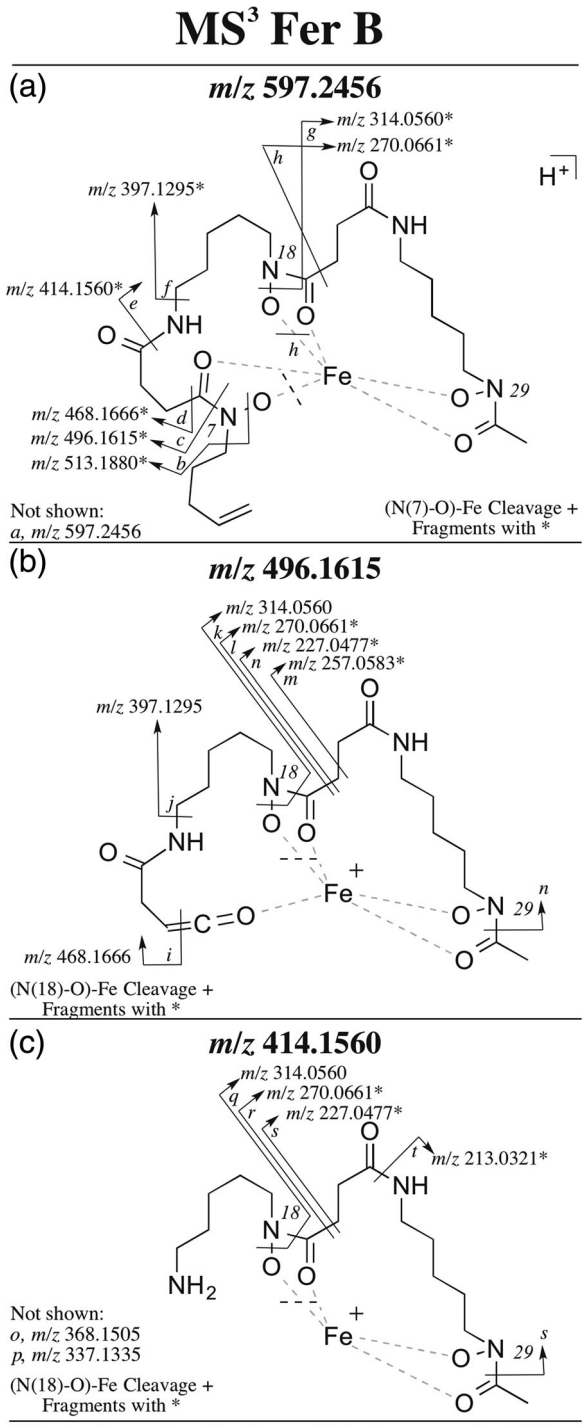

Figure 2. Fer B, top three MS^2 fragments chosen for MS^3 fragmentation and their resulting major and minor ions (theoretical *m/z* shown). Ions resulting from multiple fragmentation events are denoted with (*). Fragments not shown include: *a*, *o*, and *p*. Molecular formulas for *a* and *o* are provided in SI Table 2

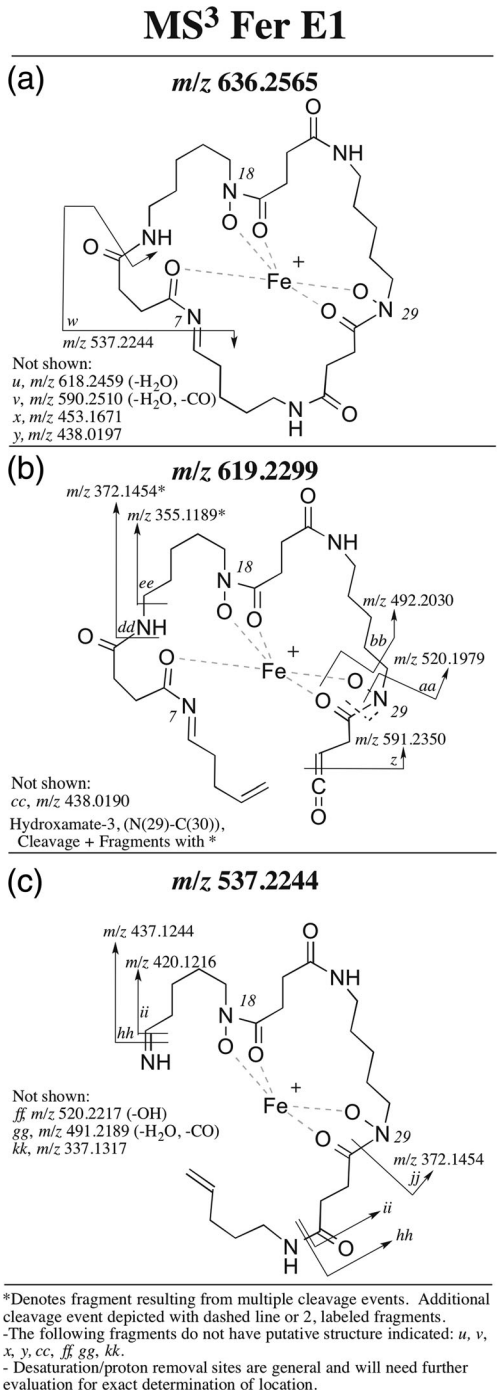

Figure 3. Fer E1, top three MS^2 fragments chosen for MS^3 fragmentation and their resulting major and minor ions (theoretical *m/z* shown). Ions resulting from multiple fragmentation events are denoted with (*). Fragments not shown include: *u*, *v*, *x*, *y*, *cc*, *ff*, *gg*, and *kk*. Molecular formulas for *u*, *v*, and *gg* are provided in SI Table 2

containing siderophores, heteroatom composition at amide, oxime, and hydroxamate linkages remain consistent between the molecular suites. Because of this, the fragments resulting from cleavage of these specific bond types were of particular interest as they can direct future structural studies based on *m/z* deviations.

Fragments arising from these bond breakage events are localized to the following regions: amide (*e*, *t*) oxime (*b-h*, *l-n*, *r-t*), and hydroxamate (*c*, *g*, *k*, *n*, *q*, *s*) (Figure 2, SI Tables 2 and 3).

Cyclized Ferrioxamine E1: MS^3

The three most abundant ions in the Fer E1 MS^2 spectra (*m/z* = 636, 619, 537) were chosen for MS^3 analysis (±0.5 Da mass selection window) (Figure 3, SI Figure 4). All detected MS^3 fragments, proposed neutral losses, and ppm deviations are summarized in SI Tables 2 and 3. Previous reports have indicated that the cyclized trihydroxamate, Fer E1, undergoes a unique combination of cleavage events compared with structurally similar, linear trihydroxamates such as Fer B [11, 12]. The expected ions from these cleavage events were observed at the MS^2 (*m/z* = 636, 619, 537) and MS^3 (*m/z* = 618, 591, 520, 437) level in this work. Similar to Fer B, high molecular weight and abundant fragments of Fer E1 were the result of water (–H_2O; *u*) or carbon monoxide loss (–CO; fragment *z*, SI Table 2, Figure 3b) from the molecular ion. As was seen with Fer B, loss of water and carbon monoxide together also yielded major species (SI Table 2, fragments *v* and *gg*). However, unlike the linear molecule, Fer E1 underwent dehydration or decarbonylation concurrent with cleavage of several other bonds (e.g., C–C, C–N; SI Table 2, Figure 3b, c fragments *aa* and *ii*). Fragment *ii* (*m/z* = 420.1202) and related species *hh* (*m/z* = 437.1226) are of particular interest because they are yielded from the cleavage of amide-3 (between C(33)-N(1)), which is present only in Fer E1 as it is the site of cyclization.

In comparison to the linear siderophore, Fer E1 underwent bond breakage between amide (*w*, *dd*, *hh*, *ii*) and C–N bonds (*w*, *aa*, *ee*, *hh*, *ii*) more frequently, whereas fragmentation between C–C bonds (*bb*) and oxime units [(N)-(O-Fe) or (N-O)-Fe, *aa*, *bb*] were less common than in Fer B. This was curious given the noncyclic structure of the MS^2 fragments of Fer E1, suggesting that MS^3 data can be correlated back to the parent geometry for the cyclized trihydroxamates. It is postulated that the cyclic, Fer E1, retains more oxime interactions because of the proximity of the Fe (III) to these units in the cyclic geometry [15]. Our data suggest that the result of these iron–oxygen interactions is less oxime breakage (*aa*, *bb*) and a variable fragmentation compared with the more flexible, linear Fer B.

Conclusion

We have annotated the first reported MS^3 profiles for ferrioxamine B and E1 for all major fragments and neutral losses with <10 ppm mass accuracy. Owing to the growing evidence that suites of trihydroxamate siderophores are present at low concentrations (<ng/L) in the iron (III) bound ($[M - 2H + Fe]^+$) state in microbial samples, the bound form and resulting tandem MS fragmentation patterns are of great significance for compound discovery. We demonstrate that cyclic and linear siderophore structures influence fragmentation patterns and are dependent on the chelation of the oxime units to iron (III). This insight will assist in future structure elucidation efforts with iron bound trihydroxamate siderophores.

Acknowledgments

We thank the Laboratory for Biological Mass Spectrometry at Indiana University for helpful experimental guidance. This work was supported by a NSF Career Award, a Cottrell Scholar Award and a Sloan Research Fellow Award.

References

1. Sandy, M., Butler, A.: Microbial iron acquisition: marine and terrestrial siderophores. Chem. Rev. **109**, 4580–4595 (2009)
2. Helman, R., Lawrence, G.D.: The increase in ferrioxamine B reduction potential with increasing acidity of the medium. Bioelectrochem. Bioenerg. **22**, 187–196 (1989)
3. Beasley, F.D., Vinés, E.D., Grigg, J.C., Zheng, Q., Liu, S., Lajoie, G.A., Murphy, M.E.P., Heinrichs, D.E.: Characterization of staphyloferrin A biosynthetic and transport mutants in *Staphylococcus aureus*. Mol. Microbiol. **72**, 947–963 (2009)
4. Cornelis, P., Dingemans, J.: *Pseudomonas aeruginosa* adapts its iron uptake strategies in function of the type of infections. Front. Cell. Infect. Microbiol. **3**, 75 (2013)
5. Martinez, J., Carter-Franklin, J.N., Mann, E.L., Martin, J.D., Haygood, M.G., Butler, A.: Structure and membrane affinity of a suite of amphiphilic siderophores produced by a marine bacterium. Proc. Natl. Acad. Sci. U. S. A. **100**, 3754–3759 (2003)
6. Martin, J.D., Ito, Y., Howmann, V.V., Haygood, M.G., Butler, A.: Structure and membrane affinity of new amphiphilic siderophores produced by *Ochrobactrum* sp. sp18. J. Biol. Inorg. Chem. **11**, 633–641 (2006)
7. Barry, S.M., Challis, G.L.: Recent advances in siderophore biosynthesis. Curr. Opin. Chem. Biol. **13**, 205–215 (2009)
8. Guaglitz, J.M., Iinishi, A., Ito, Y., Butler, A.: Microbial tailoring of acyl peptidic siderophores. Biochemistry **53**, 2624–2631 (2014)
9. Sidebottom, A.M., Johnson, A.R., Karty, J.A., Trader, D.J., Carlson, E.E.: Integrated metabolomics approach facilitates discovery of an unpredicted natural product suite from *Streptomyces coelicolor* M145. ACS Chem. Biol. **8**, 2009–2016 (2013)
10. D' Onofrio, A., Crawford, J.M., Stewart, E.J., Witt, K., Gavrish, E., Epstein, S., Clardy, J., Lewis, K.: Siderophores from neighboring organisms promote the growth of uncultured bacteria. Chem. Biol. **17**, 254–264 (2010)
11. Gledhill, M.: Electrospray ionisation-mass spectrometry of hydroxamate siderophores. Analyst **126**, 1359–1362 (2001)
12. Mawji, E., Gledhill, M., Worsfold, P.J., Achterberg, E.P.: Collision-induced dissociation of three groups of hydroxamate siderophores: ferrioxamines, ferrichromes, and coprogens/fusigens. Rapid Commun. Mass Spectrom. **22**, 2195–2202 (2008)
13. Roberts, A.A., Schultz, A.W., Kersten, R.D., Dorrestein, P.C., Moore, B.S.: Iron acquisition in the marine actiomycete genus *Salinispora* is controlled by the desferrioxamine family of siderophores. FEMS Microbiol. Lett. **335**, 95–103 (2012)
14. Groenewold, G.S., Van Stipdonk, M.J., Gresham, G.L., Chien, W., Bulleigh, K., Howard, A.: Collison-induced dissociation tandem mass spectrometry of desferrioxamine siderophore complexes from electrospray ionization of UO_2^{2+}, Fe^{3+}, and Ca^{2+} solution. J. Mass Spectrom. **39**, 752–761 (2004)
15. Spasojevíc, I., Boukhalfa, H., Stevens, R.D., Crumbliss, A.L.: Aqueous solution speciation of Fe(III) complexes with dihydroxamate siderophores alcaligin and rhodotorulic acid and synthetic analoges using electrospray ionization mass spectrometry. Inorg. Chem. **40**, 49–58 (2001)